Al-Farouk journal of sciences
Volume (2), Issue (3) (JUNE, 2026)
ISSN: 3135-2359

مجلة الفاروق للعلوم
المجلد (2) العدد 3 يونيو 2026
ردمد: 3135-2359

Removal of Methyl Violet Dye from Aqueous solutions using $AFe_{0.9}Cu_{0.1}O_3$ (A= Nd^{+3} & Eu^{+3})

Labib. A. Awin[*1], Hind. M.Ashour[2], Mahabba. M. Al-Routtoub[1] and Mahmoud. A. El-Rais[1]
[1]*Chemistry Department, Faculty of Science, The University of Tripoli , Libya*
[2] *Faculty of Science, The University of Tripoli , Libya*
Corresponding Autor**:** L.Awin@uot.edu.ly**.**

تاريخ الاستلام: 2026/04/03 تاريخ المراجعة 2026 /05/02 تاريخ القبول:2026/05/15- تاريخ النشر: 2026 /06/06

Abstract:
Two samples of nanoparticle oxides with general formula $NdFe_{0.9}Cu_{0.1}O_3$ and $EuFe_{0.9}Cu_{0.1}O_3$ were synthesized and their capabilities in the removal of Methyl Violet dye investigated. Both samples have an orthorhombic perovskite-type structure in space group *Pbnm.* The replacement of Nd^{3+} ([Xe] $4f^3$, 1.27 Å) by Eu^{3+} ([Xe] $4f^6$, 1.23 Å) has influenced removal capacities with no noticeable change in crystal size of the two oxides. The crystallite size of $NdFe_{0.9}Cu_{0.1}O_3$ and $EuFe_{0.9}Cu_{0.1}O_3$ was determined to be 56.10 and 56.40 nm respectively. The maximum removal capacity of Methyl Violet was found to be (5.75 and 0.68 mg/g) using $NdFe_{0.9}Cu_{0.1}O_3$ and $EuFe_{0.9}Cu_{0.1}O_3$ respectively. The batch mode study showed that the removal percentage increased as pH increased using $EuFe_{0.9}Cu_{0.1}O_3$ but contributory decreased using $NdFe_{0.9}Cu_{0.1}O_3$. This could be attributed to differences in the electron configurations of the *A* site cations. The removal of Methyl Violet using both two oxides has a negative relationship with temperature an ionic strength but steadily increases as contact time increased.
Keywords: Removal, Methyl Violet , Perovskite oxide, *A*- site Cation.

Introduction:

Methyl Violet (MV) as a cationic water soluble synthetic dye exposes the aquatic ecosystem for a potential hazardous pollution. It is none biodegradable, disrupts photosynthesis reactions by blocking the light and increasing chemical oxygen demand. It is a mixture of tetra, penta and hexamethyl paraarosanilins utilized in textiles, paper and bacterial gram staining[1]. The emission of such dye from industrial activities causes degradation of water quality, thus several techniques were reviewed to eliminate such pollutant. These techniques can be classified to physical processes such as adsorption, chemical treatments such as bleaching and other such as photo degradation [3, 4]. Adsorption has shown high efficiency in the wastewater treatment and the water purification. It can produce economically high quality water is sufficient time[5, 6].

In recent decades, many researches focus on developing new adsorbents with unique properties and functionalities to enhance the adsorption process. That depends on the characteristics of adsorbents such as surface area, porosity, size distribution and surface charge. Perovskite type oxides with general formula ABO_3 are expected to be good candidates for dyes removal. They are highly versatile due to the flexibility in the chemical composition with a large number of cations[7]. Those cations can fit into both the *A* and *B* positions within the same crystalline structure. Perovskite oxides that contain a lanthanide element at position *A* and a transition metal at position *B* are used more frequently in heterogeneous catalysis, obviously exploiting the catalytic properties of transition metals. [7, 8]. This work investigates the capability of the disordered double perovskite $EuFe_{0.9}Cu_{0.1}O_3$ and $NdFe_{0.9}Cu_{0.1}O_3$ in the

removal of Methyl Violet dye from aqueous solutions. In this perovskite structure, the two smallest cations (Fe/Cu) will sit in the octahedral sites, whilst the largest cation (Eu or Nd) will occupy the 12-coordinate (cuboctahedral) site. Doping Cu^{2+} into $AFeO_3$ (A= Eu^{+3} , Nd^{+3}) is expected to enhance the adsorption properties of the two oxides as result of introducing electron holes on the *A* site of structure. These holes are created by the oxidation of the *A* site cation from 3+ to 4+ which is vital to neutralize the overall charge of the oxides. The replacement of Eu^{3+} by Nd^{3+} is also expected to impact the properties due to the differences in electron configurations and ionic size of the two cations.

Experimental

Sample preparation

The preparation of two samples involved different stoichiometric compositions of Nd_2O_3 (Koch-Light Laboratories, 99.99%), Eu_2O_3 (Riedel-de Haën, 99.9%), $Cu(NO_3)_2{\cdot}3H_2O$ (J.T. Baker Chemical, 99.9%) and $Fe(NO_3)_3{\cdot}9H_2O$ (J.T. Baker Chemical, 99.9%). The mixtures were initially ground and preheated at 250°C for 12 h, and then reground and heated at following stages: 850°C for 24h, 1000°C for 48h, 1050°C for 24 h and 1100°C for 48 h.

Instrumentations

The crystallography of the samples was examined by a PANanlytical EMPYREA X-ray powder diffraction using Cu Kα radiation (1.5400 Å) and a PIXcel solid-state detector. the operating voltage was 40kV and the current was 30 mA. The samples were measured in lat plate mode at room temperature with a scan range of $10°<2\theta<80°$ and a scan length of 10 mins were used. The structures were matched using the high score program.

The absorbance of MV solutions was determined using ultraviolet visible spectrophotometer (model UV754N) at maximum wavelength of absorbance (590 nλ). The concentrations of solutions were estimated from the concentration dependence of absorbance fit. The pH measurements were carried out on a WTW720 pH meter model CT16 2AA (LTD Dover Kent, UK) and equipped with a combined glass electrode.

Batch mode

Batch mode removal studies were carried out by varying several parameters such as contact time, pH, temperature and mass of prepared oxide (adsorbent). Essentially, a 50 ml of dye solution with concentration of 10 ppm was taken in a 250 ml conical flask in which the initial pH was adjusted using HCl/NaOH. Optimized amount of adsorbent was added to the solution and stirred using magnetic stirrer for specific time. The oxide samples were separated from solutions using centrifuge 4000 CPM for 5 minutes.

3- Result and discussions:

3.1. Characterization of oxides

The chemical synthesis using solid state reaction aids to study the impact of altering the chemical composition on the physical properties. The heating regime described in previous section produced crystalline, black and greenish coloured, samples for $NdFe_{0.9}Cu_{0.1}O_3$ and $EuFe_{0.9}Cu_{0.1}O_3$ respectively. X-ray diffraction measurements (Figure 1) show the samples to be crystalline and the data are consistent with these all having an orthorhombic structure with space group (*Pbnm*). The XRD patterns exhibited $NdFe_{0.9}Cu_{0.1}O_3$ to have a single phase structure and crystallinity with higher degrees than those for $EuFe_{0.9}Cu_{0.1}O_3$. Both the shape and the size of particles are defined by the synthesis methods; however the ratio of nucleation to growth rates of particles is also important. Each of these processes depends in turn on variations in the reaction conditions such as the temperature and the nature of metals. The differences in the crystallinity of the two oxides could be attributed to one of these variations.

The solid state chemistry of Nd^{3+} (8 coordinate ionic radius , 1.27 Å)[9] and Eu^{3+} (8 coordinate ionic radius, 1.23 Å)[9] are generally believed to be quiet similar, so it is reasonable to expect $NdFe_{0.9}Cu_{0.1}O_3$ will display similar behaviour to $EuFe_{0.9}Cu_{0.1}O_3$. The crystallite size of $NdFe_{0.9}Cu_{0.1}O_3$ (56.03 nm) is found to be similar to that for $EuFe_{0.9}Cu_{0.1}O_3$ (56.34 nm). This

reflects the similarity in the ionic radii of both Nd^{3+} (1.27 Å) and Eu^{3+} (1.23 Å) cations. The average crystallite size D_p, specific surface area S, lattice strain φ estimated from X-ray diffraction data are summarised in Table-1. The crystallite size can be calculated using sheerer formula[10] (Equation. 1) where the specific surface area can be calculated using Sauter formula[11] (Equation.2) in which ρ is the density of the synthesised material.

$D_p = (0.94\lambda)/(\beta_{1/2} \times \cos\Theta)$. (1)

$S = 6000/ (D_p \times \rho)$. (2)

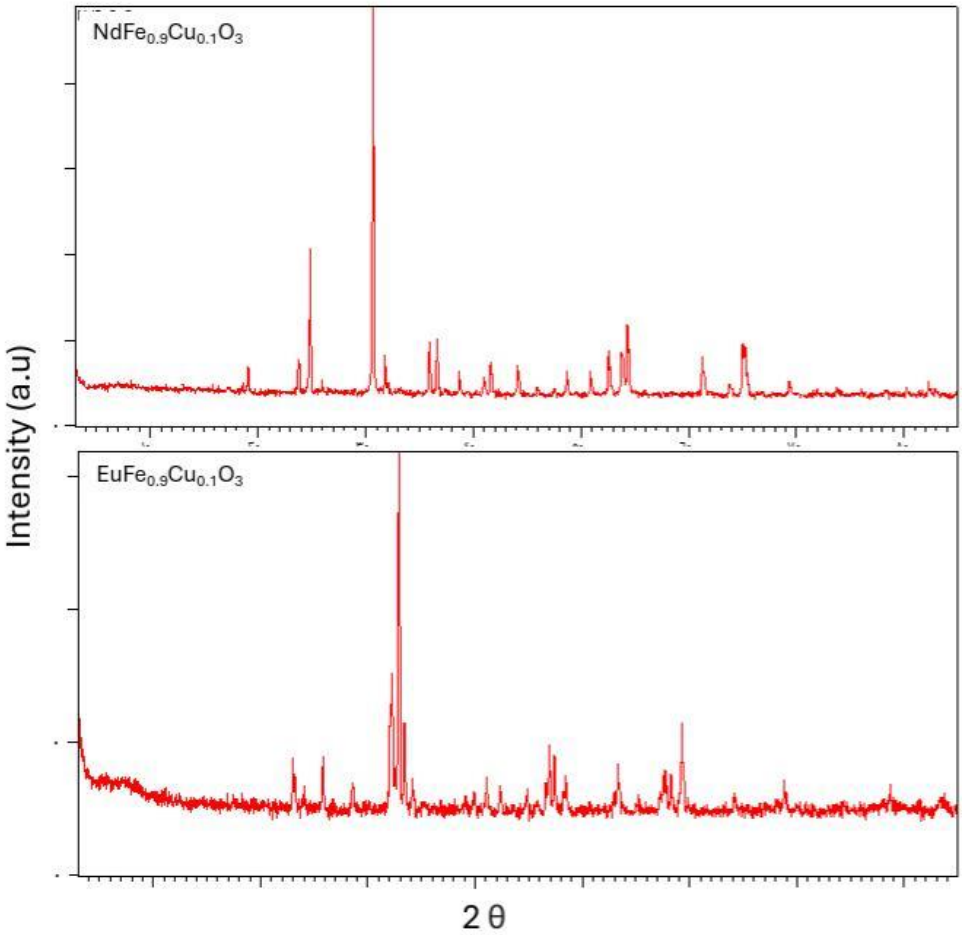

Figure 1 the XRD patterns of $NdFe_{0.9}Cu_{0.1}O_3$ and $EuFe_{0.9}Cu_{0.1}O_3$.

Table-1; Average Crystallite size D_p, Specfic surface area S, lattice strain φ, Lattice parameter *a* and Cell volume V. estimated from X-ray diffraction data.

Formula	D_p (ηm)	$\rho(g/cm^3)$	$S (m^2/g)$	φ
$NdFe_{0.9}Cu_{0.1}O_{3.5}$	56.03	6.90	15.15	0.00244
$EuFe_{0.9}Cu_{0.1}O_3$	56.34	7.18	14.82	0.00226

3.2. Batch mode

3.2.1 Effect of Time.

The removal percentage of dyes over the adsorbents can be calculated as: $R\% = [(C_i-C_t)/C_i] \times 100$, where R% is the removal percentage, $C_i = 10$ ppm is initial concentration of dye solution, C_t is the concentration of dye at contact time estimated from the concentration dependence of absorbance fit. Figure 2. shows the time dependence of MV removal at room temperature.

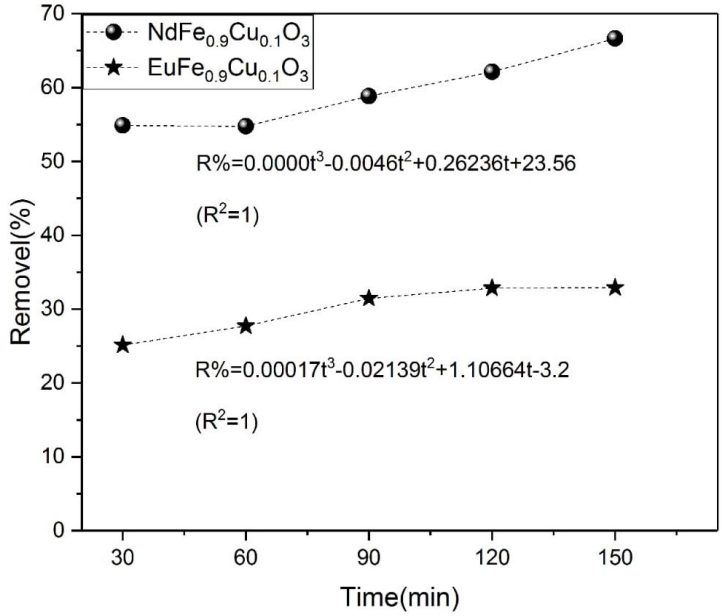

Figure 2. The time dependence of MV removal at room temperature. The volume, concentration and pH of the dyes solution are 50ml, 10ppm and 5 respectively.

There is no finite time was observed for the dye removal up to 150 min. The removals of the dye increase as the contact time increases. The removal of MV on the surface of $NdFe_{0.9}Cu_{0.1}O_3$ (66.63%) was approximately two times greater than that of $EuFe_{0.9}Cu_{0.1}O_3$ (32.90%). This result neglects the impact of the crystallite size on the adsorption properties. The removal of the organic dye is likely affected by the electron configurations of the *A* site cations. The electronic structure of $NdFe_{0.9}Cu_{0.1}O_3$ and $EuFe_{0.9}Cu_{0.1}O_3$ is anticipated to be different due to the differences in the number of *f* electron for Nd^{3+} ([Xe] $4f^3$) and Eu^{3+} ([Xe] $4f^6$). The inserted two equations in the figure give the relationships between removal percentage and contact time for each oxide. These equations were estimated from the time dependence of removal fit. The initial rate of removal for each oxide can be calculated from the first derivation of the two equations when t = 0. The initial rates of MV removal are found to be 0.26236 and 1.10664 min^- using $NdFe_{0.9}Cu_{0.1}O_3$ and $EuFe_{0.9}Cu_{0.1}O_3$ respectively.

3.2.2: Effect of adsorbent mass:

The amount of the dye adsorbed by one gram of the oxides (Q) was calculated as following: $Q\ (mg/g) = [(C_i-C_t)\times V]/W$, where t= 150 min is the contact time, V= 50 ml is the volume of MV solution and W is the mass of oxides. As shown in Figure 3, Q decreases as the mass of adsorbents increased.

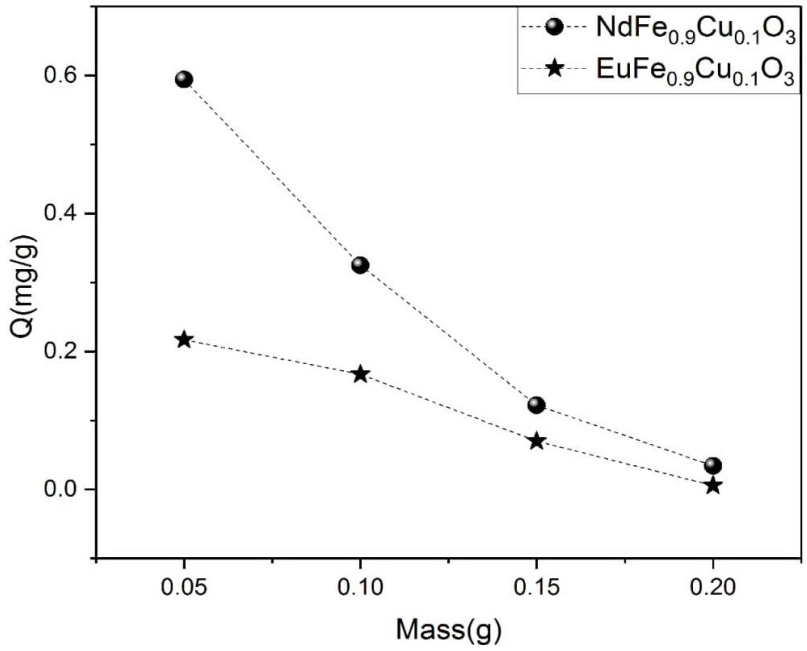

Figure 3 The effect of adsorbent mass on the removal. The time, volume, concentration and pH of dye solutions are 150min, 50ml, 10ppm and 5.1 respectively.

The maximum capacity of adsorbent Q_{max} can be estimated from the intercept of the liner fit of $1/Q_t$ at Y axis. Despite the similarity of crystallite size, $NdFe_{0.9}Cu_{0.1}O_3$ exhibited a value of Q_{max} (5.76 mg/g) greater than that for $EuFe_{0.9}Cu_{0.1}O_3$ (0.68 mg/g) at room temperature. This result is consistent with the similarity in the cell volumes of the two oxides The removal capacity of Methyl Violet is lower than those recorded for Methyl violet when the perovskite oxides $BaSr_2NbO_{5.5}$ (~9.3 mg/g)[12], $Sr_2CaNbO_{5.5}$ (47.39 mg/g)[13] and AgNPs (49.63 mg/g) [14] were used as adsorbents. The time dependence of removal capacity for each absorbent mass is illustrated in Figure 4. Based on the time dependence of removal fit for each oxide mass, the initial rates of removal were estimated as mentioned in section 3.2.1, and found to be positive correlated with the increase in oxide mass. For example, the initial rates of removal were found to be 0.0961, 0.26236, 0.3119 and 0.6673 min^- using 0.05, 0.1, 0.2 and 0.25 g of $NdFe_{0.9}Cu_{0.1}O_3$. This means the initial rate of removal increased gradually as the oxide mass increased.

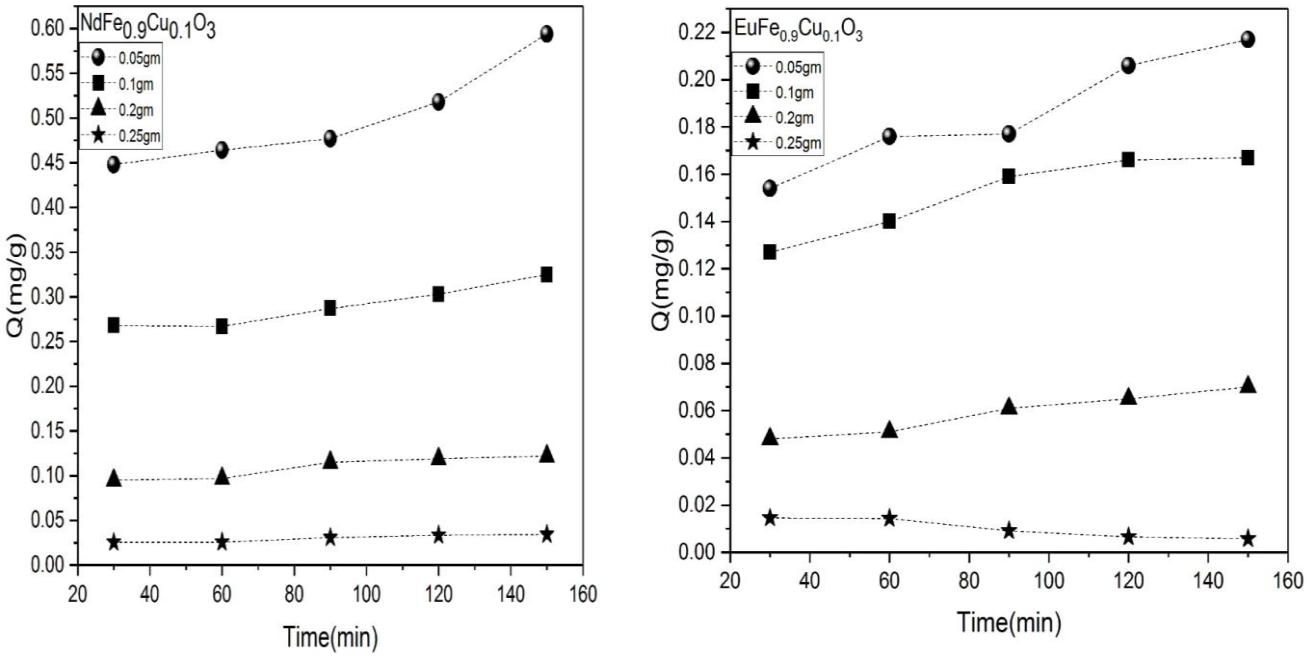

Figure 4 The Time dependence of removal capacity for each oxide mass. The volume, concentration and pH of dye solutions are 50ml, 10ppm and 5.1 respectively.

3.2.3: Effect of temperature:

Temperature has an important impact on the adsorption process. An increase in temperature helps the reaction to compete more efficiently with e^-/H^+ recombination. The removal of MV dye was investigated at 25, 40, 60, 80 and 100°C. The obtained results are illustrated below in Figure 5. The removal of MV dye decreased as temperature increased on both the two oxides surfaces. For instance, the removal of MV decreased from ~62.6% at 25°C to ~17.7% at 100°C on $NdFe_{0.9}Cu_{0.1}O_3$ surface. This result is disagreed with normal expectations, and is probably a consequence of an increase in the thermal energy. It is anticipated that higher temperature induces higher mobility of active sites of adsorbents and the surface area is decreased by increase the temperature[15]. Remarkably, the removal percentage of MV dye using the perovskite oxide ($EuFe_{0.9}Cu_{0.1}O_3$) kept relativity constant up to 60 °C and then gradually decreased up to 100 °C. Such behaviour could be attributed to the activation energy of the reaction. The energy of activation (E_a), was calculated from the Arrhenius plot of ln R % vs 1/T (Figure 6). Arrhenius plot shows that the activation energies of the removal are negative and equal to -17.38 and -18.16 kJ/mole for $NdFe_{0.9}Cu_{0.1}O_3$ and $EuFe_{0.9}Cu_{0.1}O_3$ respectively. This reflects the similarity in the strength of the interaction forces between the dye and the two oxides. The $EuFe_{0.9}Cu_{0.1}O_3$ exhibited higher exothermic energy than that for $NdFe_{0.9}Cu_{0.1}O_3$

is corresponded to the increase in the *f* electrons of the *A* site cations Nd^{3+} ([Xe] $4f^3$) and Eu^{3+} ([Xe] $4f^6$).

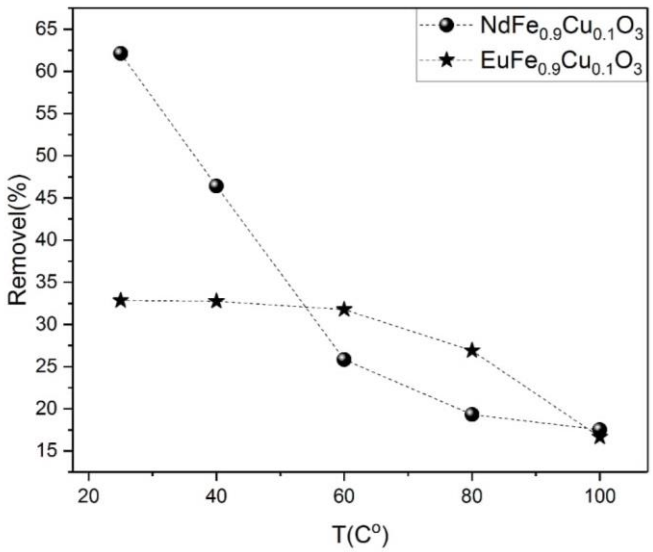

Figure 5. the temperature dependence of the MV removal. The time, volume, pH and concentration of dyes solutions are 150min, 50ml, 5.1 and 10ppm respectively

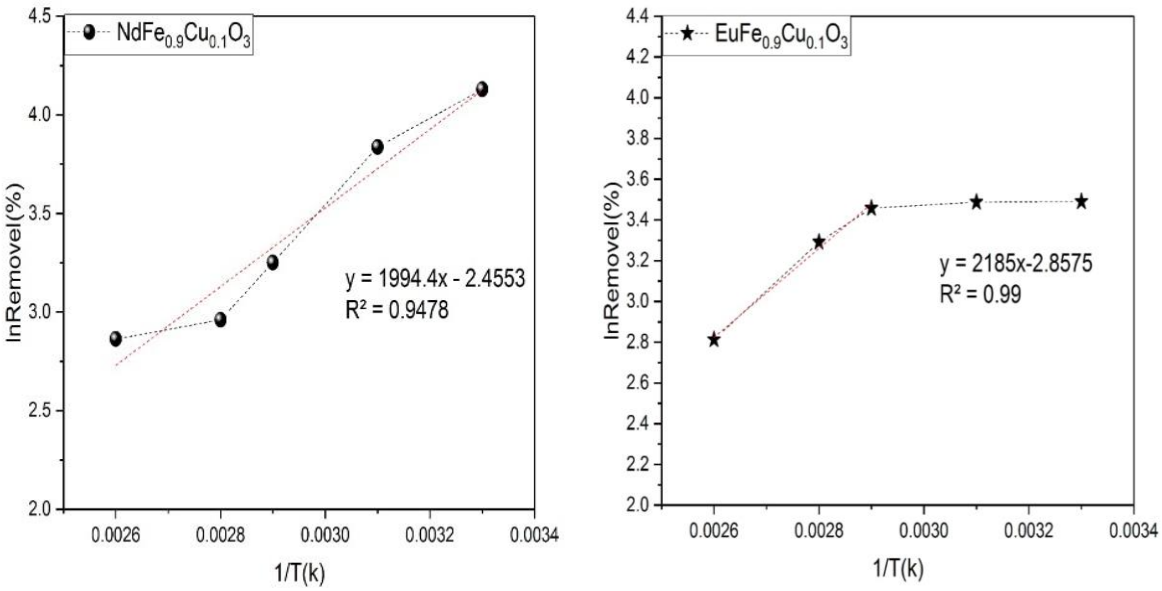

Figure 6. The Arrhenius plot of ln R % vs 1/T. The time, volume, pH and concentration of dyes solutions are 150min, 50ml, 5.1 and 10ppm respectively.

3.2.4: Effect of pH:

The pH of solutions is a key parameter in dye adsorption. The magnitude of electrostatic charges which are impacted by the ionised dye molecules is controlled by the solution pH. As a result the rate of adsorption will vary with the pH of the medium used. In general, at low

solution pH, the percentage of dye removal will decrease for cationic dye adsorption, while for anionic dyes the percentage of removal will increase. This is due to the increase in the positive charge on the solution interface and the adsorbent surface. In contrast, high solution pH is preferable for cationic dye adsorption but shows a lower efficiency for anionic dye adsorption. The positive charge at the solution interface will decrease while the adsorbent surface appears negatively charged [16].

To study the effect of pH, experiments were carried out at various pH values, ranging from 2 to 8 for constant dye concentration (10 ppm) and adsorbent mass (0.1g). Figure 6 presents the

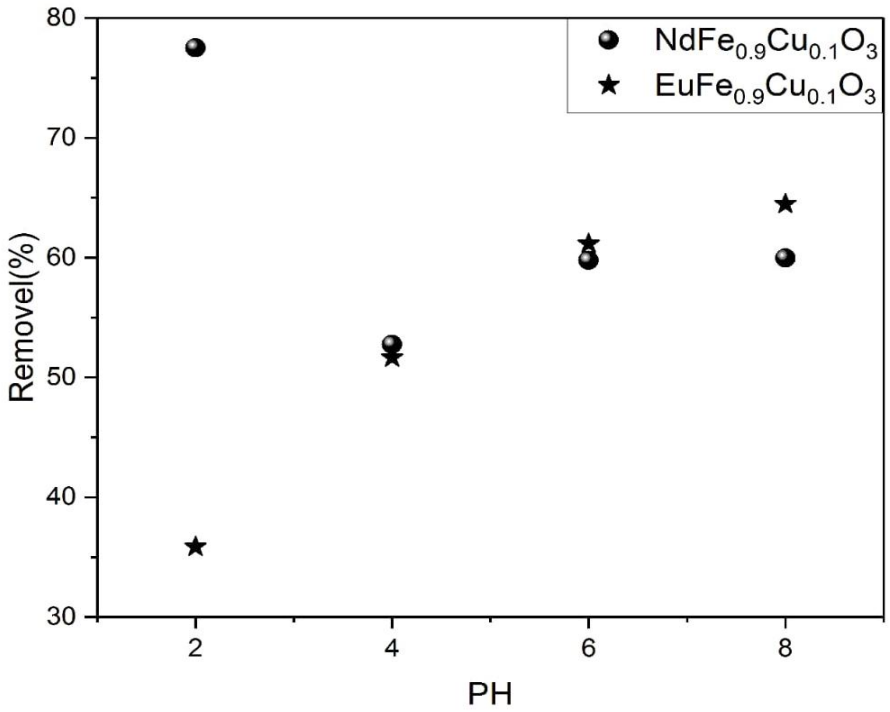

removal of dyes as a function of pH.

Figure 6. The pH dependence of the MV removal. The time, volume and concentration of dyes solution are 150 min, 50ml and 10ppm respectively.

It was observed that the removal of MV using the $NdFe_{0.9}Cu_{0.1}O_3$ slightly decreases as pH increased, while the dye removal on the surface of $EuFe_{0.9}Cu_{0.1}O_3$ increased as pH increased. The highest removal of MV was recorded at pH= 2 for $NdFe_{0.9}Cu_{0.1}O_3$ (~ 78 %) and pH=8 for $EuFe_{0.9}Cu_{0.1}O_3$ (~ 64 %). This reflects the role of *f* electron for *A* site cations in the adsorption process. The removal efficiency of the two adsorbents seems to be similar at pH=4 and 6 where at pH=2 remarkable differences (≤20 %) can be noticed.

3.2.5: Effect of ionic strength :

The ionic strength of a solution influences the chemical system in which the activity coefficient of ions decreases as the total of ions concentrations increases. The solubility of salts and the rate of reactions are also affected in which the last can be either positive or negative correlated with the ionic strength depending on the ionic charge. Hence, the ionic strength effect on adsorption process was investigated by adding 0.1, 0.2 and 0.3 g of NaCl to the dye solutions.

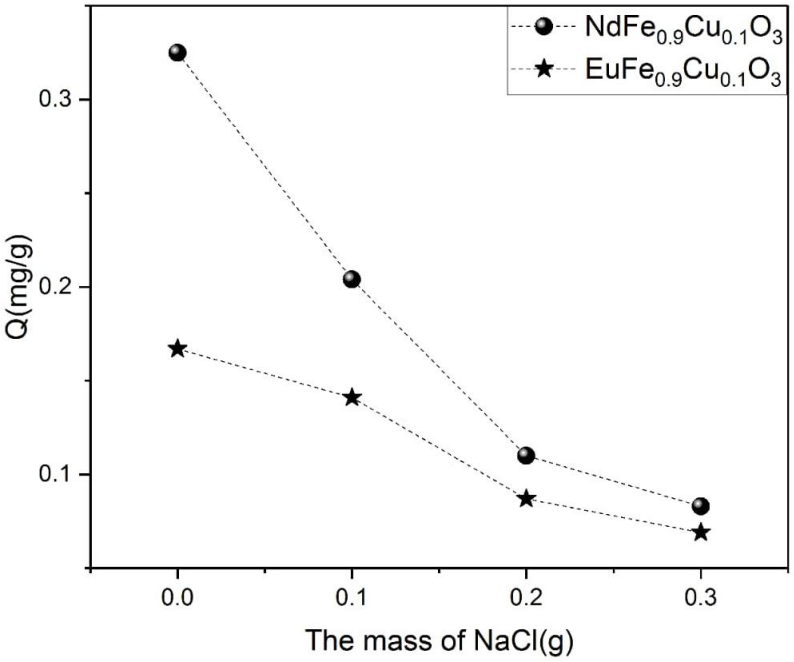

Figure 7 The ionic strength effect on the MV removal. The time, volume, pH and concentration of dyes solution are 150 min, 50ml, 5 and 10ppm respectively.

As presented in Figure 7, the absorbed amount of MV dye decreased as the mass of NaCl increased using both the two oxides. The increase of the ionic strength resulted in a decrease in the dye removal. The finding corroborates with what reported by Bayramoglu et al (2009) **[17];** and reflects the importance of electrostatic interaction between dye molecules and the two oxides. The theory beyond such behavior stems from the role of electrical double layer on the absorbent surfaces. The salt concentration influences the diffuse part of the electrical double layer, which in turn affects the surface charge**[18][19].** The increase in Na^+ ions concentration may screen the negatively charged oxides surface, leading to the reduction of the cationic dye adsorption**[20].** The following equation expresses the relationship between dye removal capacity and the added mass of NaCl (X *in g)*:

Q (mg/g) = 0.2881- 0.745X (using $NdFe_{0.9}Cu_{0.1}O_3$).

Q (mg/g) = 0.1675- 0.345X (using $EuFe_{0.9}Cu_{0.1}O_3$).

The slope of the first equation is slightly double of that for the second. This "again" is correlated with the number of *f* electrons for the *A* site cations.

4- Conclusion:

The removal of Methyl Violet from aqueous solution by the nano particle oxides $NdFe_{0.9}Cu_{0.1}O_3$ and $EuFe_{0.9}Cu_{0.1}O_3$ has been reported. The two oxides were synthesised by solid state reaction and characterized by XRD. Despite the similarity in crystallite size, the adsorbed mounts of MV by them were different. The replacement of Nd^{3+} ([Xe] $4f^3$) by Eu^{3+} ([Xe] $4f^6$) resulted in higher removal capacity and lower exothermic activation energy as the number of *f* electrons of the *A* site cations decreased. This reflects the critical role of the electron configurations for the two cations in adsorption process. The maximum removal capacities of Methyl Violet are 5.76 and 0.68 mg/g for $NdFe_{0.9}Cu_{0.1}O_3$ and $EuFe_{0.9}Cu_{0.1}O_3$

respectively. The removal of dye gradually increased as time increased but decreased as temperature and the ionic strength increased. The removal of MV was positively correlated with pH using $EuFe_{0.9}Cu_{0.1}O_3$, but it was negatively correlated on the surface of $NFe0d_{.9}Cu_{0.1}O_3$.

Acknowledgment:
The authors thank Petroleum Research Centre/ Tripoli/Libya for its assistance in XRD measurements.

5- References:

[1] Sabnis R. W (2010) Handbook of Biological Dyes and Stains: Synthesis and Industrial Applications, John Wiley and Sons. https://onlinelibrary.wiley.com/doi/book/10.1002/9780470586242.
[2] Sabnis R. W. (2007) Handbook of Acid-Base Indicators, CRC Press. https://www.perlego.com/book/1628506/handbook-of-acidbase-indicators-pdf.
[3] Cheremisinoff N. P.(2002) Handbook of Water and Wastewater Treatment Technologies, Butterworth-Heinemann.https://www.sciencedirect.com/book/monograph/9780750674980/handbook-of-water-and-wastewater-treatment-technologies. html
[4] Tushar Kanti Sen (2015) Physical, chemical and biological Treatment Process for Water and Wastewater, Nova.https://novapublishers.com/shop/physical-chemical-and-biological-treatment-processes-for-water-and-wastewater. html
[5] Pawan K. R. (2026) Adsorbents for Water and wastewater treatment and Resource Recovery , Springer Nature Switzerland. https://books.google.com.ly/books/about/Adsorbents_for_Water_and_Wastewater_Trea. html
[6] Chi Tien (2019) Introduction to adsorption (Basic, Analysis and Applications), Elsevier. https://books.google.com.ly/books/about/Introduction_to_Adsorption. html
[7] Junjiang Zho etal (2014) Perovskite Oxides: Preparation, Characterizations and Applications in Heterogeneous Catalysis, ACS Catal, 4(9) 2917-2940 . https://pubs.acs.org/doi/10.1021/cs500606g.
[8] Ishihara T. (2009) Structure and Properties of Perovskite Oxides, Springer. https://link.springer.com/chapter/10.1007/978-0-387-77708-5_1.
[9] Shannon R. D.(1970) "Cell dimensions of rare earth orthorhodites", Acta Crystallographica Section B, 26 (4) 447-449. https://doi.org/10.1107/S0567740870002613.
[10] Langford J. I. and Wilson, A. J. C. (1978) "Scherrer after sixty years: A survey and some new results in the determination of crystallite size", Journal of Applied Crystallography, 2(11) 102-113. https://doi.org/10.1107/S0021889878012844.
[11] Nogi K., Hosokawa, M., Naito, M. and Yokoyama, T.(2012) Nanoparticle Technology Handbook, Elsevier. https://books.google.com.ly/books/about/Nanoparticle_Technology_Handbook.html.
[12] Labib A Awin, M.ahmoud. A. E lRais, Enas I Baghni and Abdunnaser M Etorki,(2018) "Removal of Methylene Violet from Aqueous Solutions Using BaSr2NbO5.5", Journal of Analytical & Bioanalytical Techniques, 5 (8) 338-345. DOI: 10.4172/2155-9872.1000385.
[13] Labib. A. Awin, Mahmoud. A. El-Rais, Abdunnaser M Etorki, Mokhtar M Abobaker, Mawada. S. Alzorgani, Maryam M. Alnaas, Miloud E Sweesi and Ashraf M. Ward (2021) Removal of Methyl Violet from Aqueous Solutions using $Sr_2ANbO_{5.5}$ (A= Ca^{+2}, Sr^{+2} & Ba^{+2}), International Journal of progressive sciences and technologies, 26 (1) 67-73. https://ijpsat.org/index.php/ijpsat/article/view/2973.

[14] Mohanad El- Harbawi.etal, (2025) Removal of Methyl Violet using synthesizing silver nanoparticles from plant based biomass: Adsorption and photocatalytic degradation , Deslanition and water Treatment, 323, 101349. https://www.sciencedirect.com/science/article/pii/S1944398625003650.
[15] Michael Mozurkewich S. W. B.(1984) "Negative activation energies and curved Arrhenius plots. 1. Theory of reactions over potential wells", Journal of Physics and Chemistry, 88 (25) 6429. https://pubs.acs.org/doi/10.1021/j150669a073.
[16] Soumi Dutta etal, (2021) Recent Advances on the Removal of Dyes from Wastewater Using Various Adsorbents , Materials Advances, 14, 4497-4531. https://doi.org/10.1039/d1ma00354b.
[17] Bayramoglu et al (2009) Adsorption Kinetics and Thermodynamics Parameters of Cationic Dyes From Aqueous Solutions by Using A Strong Cation Exchange Resin, Chemical Engineering Journal, 152(2-3)339-346. https://www.sciencedirect.com/science/article/abs/pii/S1385894709003246.
[18] Islem Louati etal, (2015) Effect of Ionic Strength on the Ion Exchange Equilibrium between AMX Membrane and Electrolyte Solutions, Water Quality Research Journal, 51(1)60-68. https://iwaponline.com/wqrj/article/51/1/60/21631/Effect-of-ionic-strength-on-the-ion-exchange.
[19] Virga, E., Spruijt, E., de Vos, W.M., Biesheuvel, P.M., (2018) Wettability of Amphoteric Surfaces: The Effect of pH and Ionic Strength on Surface Ionization and Wetting. Langmuir : the ACS journal of surfaces and colloids. 34(50), 15174-15180. https://doi.org/10.1021/acs.langmuir.8b02875.
[20] Azouz, A., Fawzi, M., Mohammed, I., Hamed, O., Maher, A., & Baddi, M. (2026). Influence of Electrolyte Chemistry and Electrode Material on Hydrogen Production Performance in Alkaline Water Electrolysis. *Al-Farooq Journal of Sciences*, *2*(2), 49-66.
[21] Tholiso Ngulube etal, (2017) An Update on Synthetic Dyes Adsorption onto Clay Based Minerals: A state of art review, Journal of Environmental Management, (191) 35-57. https://www.sciencedirect.com/science/article/abs/pii/S0301479716310118